

Original Article

Mobile Solar Charging Station for Mini Electric Vehicles in Kuwait: Optimization and Economic Analysis Using HOMER Simulation Software

Jasem Alazemi¹, Jasem Alrajhi², Ahmad Khalfan³, Khaled Alhaifi⁴

^{1,2,3,4}Department of Automotive and Marine Engineering Technology, College of Technological Studies(PAAET), Kuwait.

¹Corresponding Author : jm.alazmi@paaet.edu.kw

Received: 29 October 2024

Revised: 15 December 2024

Accepted: 31 December 2024

Published: 25 February 2025

Abstract - This study uses HOMER simulation software to present the optimization and economic analysis of a mobile solar charging station for Mini Electric Vehicles (MEVs) in Kuwait. The primary goal is to design a mobile solar charging station that serves rural areas lacking infrastructure, aligning with Kuwait's Vision 2035 for sustainable energy and pollution reduction. MEVs have gained popularity in India, China, the Association of Southeast Asian Nations, and other countries. These vehicles are well suited for rapid transportation between classrooms, hospital transfers, and special events on a busy campus, as well as firefighting, ambulance, and medical assistance. The station is expected to produce approximately 15.2 kilowatt-hours per day, serving three vehicles with a 10-kW engine, each travelling 30 km/day. The system integrates solar photovoltaic panels with battery storage to create a self-sufficient charging station that can operate in remote areas. By comparing several system configurations using HOMER, this study identifies the most cost-effective design, considering factors such as energy production, battery autonomy, station weight, and installation area. The results highlight the potential of solar-powered MEV charging stations to support sustainable transportation in Kuwait, especially in regions with high solar radiation.

Keywords - Battery bank, HOMER simulation, Mini Electric Vehicles, Renewable energy, Solar EV charging station.

1. Introduction

Mini-Electric Vehicles (MEVs) have gained popularity in recent years, notably in China, India, and the Association of Southeast Asian Nations (ASEAN). MEVs are enclosed vehicles that are smaller than traditional automobiles [10]. The fundamental component of an MEV is an electric motor, as opposed to an Internal Combustion Engine (ICE), which produces power by burning fuel and gases. Thus, MEVs no longer depend on any form of conventional fuel, which results in zero emissions [11]. As a result, they do not produce air and noise pollution [20]. Therefore, using MEVs to replace conventional ICE vehicles can guarantee and preserve environmental purity [11].

The typical range of MEVs is around 110 km, with a maximum speed between 30 to 60 km/h [1, 2]. In China, it is estimated that more than 600,000 MEVs were sold in 2015; in Shandong Province alone, 610,000 MEVs were sold in 2016 [14]. In 2023, a total of 19 million two-wheeled and three-wheeled vehicles were sold in the main global markets, including China, India, and ASEAN [20]. MEVs are classified into three basic categories: two-wheeled electric scooters, three-wheeled electric rickshaws, and four-wheeled

electric vehicles [1, 3, 13]. MEVs are equipped with substantial battery bank capacity, reaching up to 350 Ah and 48-72 V, using either DC or AC motors, depending on the vehicle's size and appropriate chargers and connections [2, 13]. MEVs are designed not only for passenger transport but also for conveying merchandise, equipment, tools, and heavy loads (up to 1,630 kg) [2, 16]. Consequently, they are utilized in diverse locations such as airports, resorts, golf courses, and major hospitals.

MEVs can be customized to meet a fleet's specific needs, including security, ambulance services, or grounds maintenance. Furthermore, they can be equipped with tools, such as pallet forks or ploughs, or extended platforms to facilitate the transportation of larger equipment and to execute a variety of duties that are beyond the capabilities of many larger vehicles (such as operating in narrow streets and areas) [2, 16].

In addition to all the advantages, MEV manufacturers have ensured that driving MEVs is simple for people who own electric vehicles [11]. MEVs can be charged at home, at workplaces, or during users' own time and convenience [15,



4]. However, the infrastructure and charging stations for MEVs remain insufficient [12], and the uncontrolled charging of a surplus of MEVs may adversely affect grid power [3, 7]. To support grid power and reduce the cost of building new infrastructure for MEV charging stations, Photovoltaic (PV) systems may be installed in several locations to provide energy for MEVs [17].











Utilizing PV power systems alone to charge MEVs can contribute to the practical use of sustainable energy sources and have environmental benefits. Table 1 presents an example of six categories of MEVs that are gaining popularity in India, ASEAN, and other countries [2, 12]. Some of these MEV types are already being used in Kuwait. MEVs use electrical motors, whose power ranges from 1.5

kW up to 10 kW, and are powered by lead-acid or lithium-ion batteries with capacities ranging from 120 Ah up to 350 Ah.

MEVs have a driving range from 60 km to 110 km, which makes them perfect for short-distance applications. MEV passenger vehicles are the most common MEV type used worldwide (with seating capacities of 4, 12, and 18).

They are ideal for quick transportation between classrooms, hospital transfers, and special events on a busy campus [2]. Other MEV types can be customized as cargo types, two-seater firefighting vehicles, or ambulances to provide medical assistance.

Table 1. Most common MEV types used worldwide [2]

	Passenger vehicles with 4, 12, and 18 seats			Riko UT	Customized MEV	
						
Seating Capacity	12 seats	18 seats	4 and 6 seats	1 seat	4 seats + cargo (1 ton)	2 seats + cargo 8-seater bus
Lead-Acid Battery	225 Ah	225 Ah	175 Ah	140 Ah	175 Ah	175 Ah/225 Ah
Lithium-Ion Battery	230 Ah	230-350 Ah	120 Ah	120 Ah	120 Ah	120 Ah
Mileage	80-90 km	80-90 km	60-80 km	100-110 km	60-80 km	60-80 km
Motor	AC 7.5 KW	AC 7.5 KW-10 kW	AC 4 KW	BLDC/PMSM 1.5 kW	AC 5KW	AC 5 KW
Charging Time	6-8 hours	6-8 hours	6-8 hours	7-8 hours	6-8 hours	6-8 hours
Steering Position	RHD/LHD available	RHD/LHD available	-	-	RHD/LHD available	-
References	[2] Our Product Range, Speedways Electric, 2024. [Online]. Available: https://speedwaysev.com/about-us					
Location in Kuwait	Murouj Farm		Basic Education College (paaet- Kuwait)			
Example of MEVs that have been used in Kuwait						
MEV Location	https://maps.app.goo.gl/BmXdPrZ1ji3Xz3aM9		https://e.paaet.edu.kw/AR/Pages/default.aspx			
References	Photos sources: Author					

2. Methodology

This research examines the design of a mobile solar charging station for three MEVs in Kuwait by using HOMER Simulation Software. HOMER is an advanced tool for the modelling and optimization of renewable energy systems. It can replicate several configurations of micro-power systems, including both grid-connected and freestanding systems. The program executes three primary functions: simulation, optimization, and sensitivity analysis.

The station's initial dimensions were intended to accommodate three vehicles; consequently, the electrical capacity of the automobiles that were utilized continuously needed to be determined. In Kuwait, the most prevalent locations for MEVs are Al-Wafra Farms and Al-Abdali Farms. Power disruptions occur during prime summer hours, and there is a severe dearth of charging infrastructure. The mobile solar charging station can be implemented in any location in Kuwait lacking in charging infrastructure.

In this research, several key input parameters were fed into HOMER to simulate the performance of the mobile solar charging station under Kuwait's environmental conditions.

HOMER then conducted a sensitivity analysis to assess how variations in input parameters affect system performance, which focuses on the following:

- **Solar Radiation Variation:** The analysis evaluated how fluctuations in solar radiation (especially during winter months) impact energy production and battery autonomy. HOMER projected the state of charge of the batteries and the potential energy deficits under different radiation levels.
- **Battery Autonomy:** The sensitivity analysis examined how different battery bank configurations influence the system's autonomy. It tested the system's ability to supply energy during periods of low solar radiation and identified the optimal battery size to avoid critical energy shortages.
- **Cost Fluctuations:** HOMER tested how changes in component costs (e.g., price of batteries or PV panels) could affect the economic viability of the system.

This research also focuses primarily on minimizing the weight and area of the stations, which are critical factors for the MEVs, as well as minimizing station costs. HOMER simulated the system after verifying the station's load requirements and component sizes, resulting in four optimized configurations. A comparison was conducted to identify the most suitable system that fulfils the station's requirements. The optimal solution was analyzed comprehensively in terms of station size, weight, power management, and overall net current cost.

- **Emissions Reductions:** The environmental benefits of each configuration were evaluated by calculating the amount of emissions avoided through the use of solar energy.

3. Case Studies

3.1. Kuwait's Location and Global Solar Density

Kuwait has summer temperatures ranging from 25 °C to over 45 °C and winter temperatures from 7°C to 27 °C, attributable to its subtropical desert climate. The solar radiation data for Kuwait, sourced from the HOMER energy website [9], indicate that the nation receives higher levels of solar radiation than other countries do, with an annual average of 5.475 kWh/m²/day. The location is next to Al-Wafra Farms, where farmers are required to convey goods over short distances by using small vehicles (28°33'52.7" North, 48°03'45.8" East). This location may be ideal for the utilization of MEVs because of the elevated amounts of solar radiation and the dry climate. The most cost-effective alternative for this location is a freestanding system that includes solar energy and battery storage, as determined by the simulation results of the station developed for optimization purposes in Kuwait.

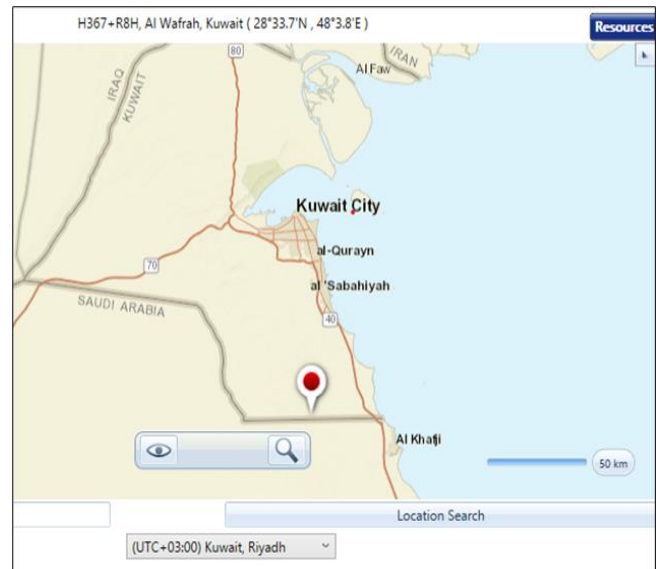


Fig. 1 Al-Wafra Farms location [9]

The HOMER global solar density map illustrates the hourly solar radiation for 2025, providing a clearer perspective on the anticipated peaks and troughs of radiation during daylight hours. Additionally, it specifies the time frame and anticipated low-radiation periods throughout the year, enabling the system to avoid crucial energy deficits in the solar system by selecting adequate energy storage solutions. Figures 2 and 3 illustrate the graph line and density map of solar radiation for the examined location, respectively.

Solar radiation demonstrated seasonal fluctuation, reaching its lowest level in winter and its highest point in summer [9]. The months exhibiting the greatest seasonal radiation are June, July, and August, with maximum global radiation levels of 0.74 kW/m²/day. December has the lowest

global radiation levels at 0.3208 kW/m²/day, followed by January at 0.3476 kW/m²/day, and November at 0.3799 kW/m²/day. The seasonal radiation for other months ranges from 0.456 kW/m²/day in February to 0.67 kW/m²/day in September.

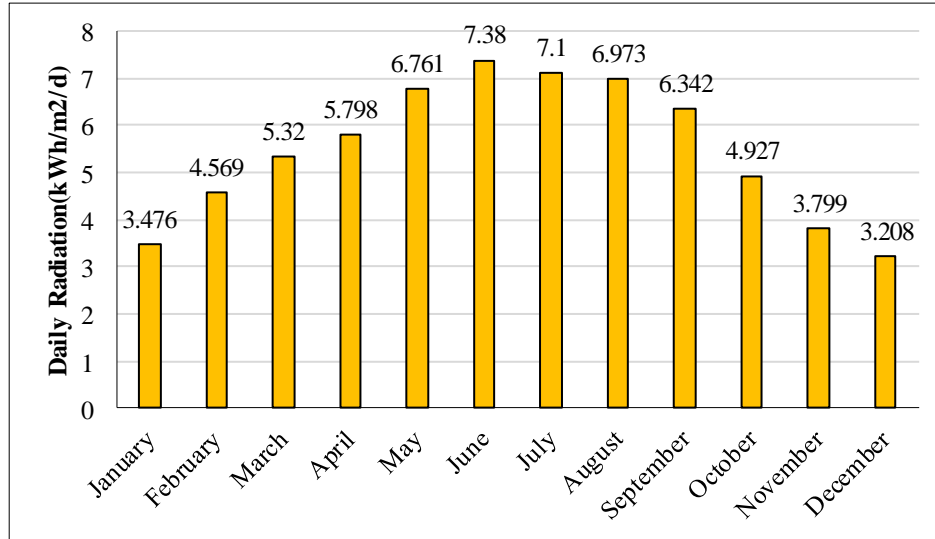


Fig. 2 Global horizontal radiation (average: 5.475 kWh/m²/d) [9]

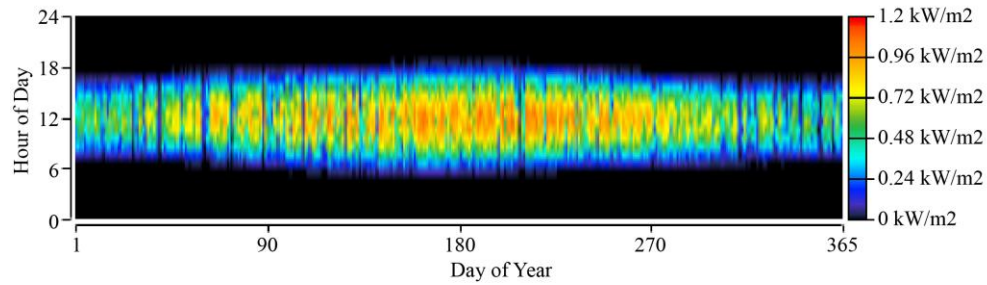


Fig. 3 HOMER global solar density map

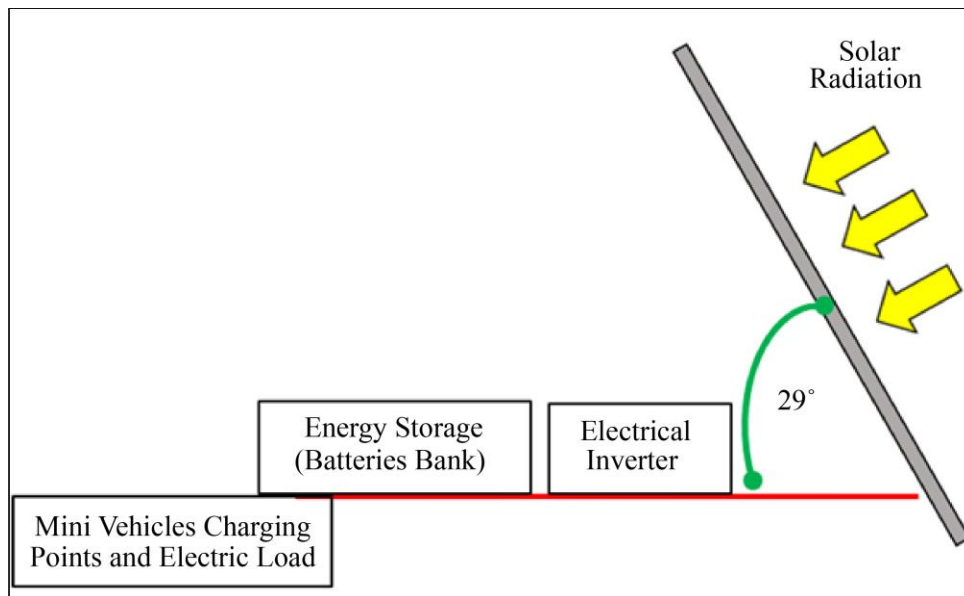


Fig. 4 Schematic of mobile MEV station components

3.2. System Design and HOMER Schematic Components

Figure 4 shows a schematic design of a charging station for MEVs. When building the PV system, it should be oriented at 0° azimuth (the PV face should be oriented toward the equator, which is the south direction) with a slope angle of 29°. This orientation will provide the highest possible energy output. Solar PV panels, an electrical inverter, a battery bank, a voltage regulator, and a charging station are the system's primary components.

Figure 5 illustrates the HOMER schematic design for the portable MEV energy system with the real annual electrical load profile. The methodology delineates the main components to be investigated to identify the optimal solution for developing a mobile MEV charging station. The figure illustrates the daily energy demands (2.5 kWh/day for system operation and 8 kWh/day for car charging), including two distinct battery types (6 and 12 V batteries) because both will be evaluated to determine the most appropriate kind, in conjunction with the inverter (Apollo S-210 and S-219C).

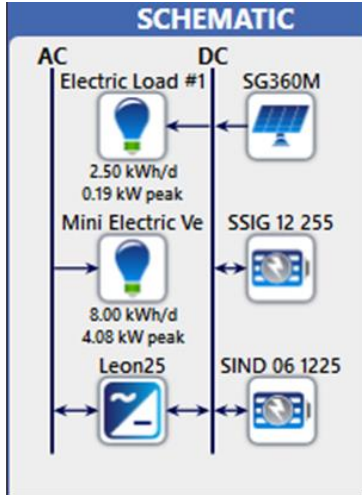


Fig. 5 HOMER schematic of the MEV charging station

3.3. Main Components of the System Model

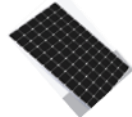
3.3.1. PV Array

The PV array serves as the primary energy source for the mobile MEV charging station. It converts solar energy into electricity, which is then used to charge the battery bank. The performance of the PV array can be affected by factors such as ambient temperature and solar radiation. HOMER calculates the output power of the solar array using the following equation:

$$P_{PV} = f_{PV} Y_{PV} \frac{I_T}{I_s} \quad [9]$$

Where P_{PV} is the PV output power, f_{PV} is the derating factor of the PV, Y_{PV} is the rated capacity of the PV array (kW), I_T is the global solar radiation, and I_s is the standard radiation used for rating the PV array (1 kW/m²).

Table 2. PV electrical characteristics [8]

	
Nominal output (Pmax)	360 W
Solar cells	72 (6 × 12) Monocrystalline Perc
Flash test power tolerance	0/+5 W
Voltage at Pmax (Vmp)	38 V
Current at Pmax (Imp)	9.48 A
Open circuit voltage (Voc)	46.6 V
Short circuit current (Isc)	10.09 A
Maximum system voltage	1500 V
Maximum series fuse rating	15 A
Module efficiency	18.54%
Dimensions	1957 × 992 × 40 (mm)
Weight	22.5 kg
Operating temperature	−40 °C to +85 °C

3.3.2. Battery Bank

The battery bank contains one or more strings of series-connected batteries and is used to store electrical energy during times of elevated PV output for subsequent usage as necessary. HOMER mimics the battery bank based on its charge and discharge capacities and durations. HOMER has a repository of physical battery characteristics, including nominal voltage, life span, capacity, lowest state of charge, and round-trip energy efficiency. New battery characteristics may be included in HOMER's library to meet the standards of the necessary battery types.

This system examines two kinds of batteries, namely, 6 and 12 V batteries, which are connected in two distinct configurations to provide 24 and 36 V outputs. The equations below illustrate the methodology used by HOMER to compute the battery bank's lifetime and the associated replacement expenses.

$$R_{batt} = \min \left(\frac{N_{batt} Q_{lifetime}}{Q_{thrpt}}, R_{batt,f} \right) \quad [9]$$

$$C_{bw} = \frac{C_{rep,batt}}{N_{batt} Q_{lifetime} \sqrt{\eta_{rt}}} \quad [9]$$

Where R_{batt} is the battery lifetime in years, Q_{thrpt} is the annual battery throughput, $R_{batt,f}$ is the battery maximum lifetime regardless of throughput, $C_{rep, batt}$ is the battery bank replacement cost, N_{batt} is the number of batteries used, $Q_{lifetime}$ is the battery lifetime in kWh, and η_{rt} is the round-trip efficiency.

Table 3. Battery specifications [18, 19]



Model	Solar SSIG 12 255	255SIND 06 1225
		
Voltage	12 V	6 V
Capacity	255 Ah	1225Ah
Dimensions (L×W×H)	380 mm × 176 mm × 373 mm	27.13 mm × 265 mm × 610 mm
Battery	Deep-cycle flooded/advanced lead-acid battery	Deep-cycle flooded/advanced lead-acid battery
Color	Maroon	Maroon
Weight	56 kg	188 kg
Cost	\$462	\$1,201.30

Table 4 shows the specifications of the Apollo S-210ia series, a single-phase grid-interactive inverter designed to function as a grid-tie inverter, hence minimizing energy use while an electric line is accessible. It has an integrated maximum power point tracking charge controller and may provide backup power from stored solar energy via its two outputs when the utility grid is inaccessible. One output supplies designated loads, while the other enables the use of solar energy without backup systems while minimizing the power transferred to the grid. It is available in 3.8- and 5.7 kW PV input configurations [5].

4. HOMER Sensitivity Case


4.1. Optimization

This research involves using HOMER for simulation, optimization, and sensitivity analysis, ultimately deriving four systems. At the start of the station design, two distinct

battery connection types were proposed to generate either a 24 or 36V supply, aimed at identifying the optimal design that aligns with the standards of the mobile MEV charging station. Figure 6 presents the HOMER data for the 24V station, while Figure 7 displays the HOMER results for the 36 V station. The findings indicate a variation in the number of components, which influences both the weight and size of the station. Weight and area are essential considerations in the design of the mobile station. A lighter weight makes relocating the station more manageable, and a smaller area facilitates installation and repairs while enhancing resistance to wind and weather fluctuations.

The HOMER results enabled determining the number of components in each design, subsequently allowing the calculation of the station's estimated weight, size, and financial cost. The following section examines the key differences between designs to identify the most appropriate design for this station

Table 4. Apollo S-210 ia S-219C IA [18]

	
Input data (DC) max. DC power	5.7 kW
Max. DC current	104 A
Output data (AC) max. AC power	5.5 kW
Nominal AC voltage	220, 230, 240 V
Frequency	50, 60 Hz
Distortion (THD)	< 3 %
No. of feed-in phases	1
Max. efficiency	96.50%
Dimensions (H/W/D)	1050 × 600 × 460 mm
Operating temperature	0 to +50 °C
Transformer	Yes
Humidity	0%-95%
Cooling	Fan
Display	LCD
Weight	144 kg

Export...		Export Details...		Optimization Results										<div><div></div> Categorized</div> <div><div></div> Overall</div>	
Double click on a system to see its Simulation Details.															
Architecture										Cost					
				SG360M (kW)	SSIG 12 255 (#)	SIND 06 1225 (#)	Leon5 (kW)	Efficiency2	Dispatch	NPC (\$)	LCOE (\$/kWh)	Operating cost (\$/yr)	CAPEX (\$)		
				7.31	10		5.00	0	CC	\$14,474	\$0.173	\$162.54	\$12,373		
				5.17		8	5.00	0	CC	\$18.125	\$0.217	\$166.84	\$15,969		

Fig. 6 24 V battery connection system


















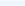
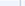

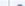
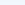
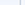


Export...		Export Details...		Optimization Results										<input checked="" type="radio"/> Categorized <input type="radio"/> Overall	
Double click on a system to see its Simulation Details.															
Architecture								Cost							
	   	SG360M (kW) 	SSIG 12 255 (#) 	SIND 06 1225 (#) 	Leon5 (kW) 	Efficiency2 	Dispatch 	NPC (\$)  	LCOE (\$/kWh)  	Operating cost (\$/yr)  	CAPEX (\$) 				
	  	6.19	12		5.00	0	CC	\$14,696	\$0.176	\$164.80	\$12,566				
	  	5.67		6	5.00	0	CC	\$16,036	\$0.192	\$165.83	\$13,892				

Fig. 7 36 V battery connection system

4.2. Winning System Specification (24 and 36 V Battery Bank Connection System)

Table 5 illustrates the characteristics of the battery bank for the four optimized systems, such as the number of batteries, total weight, number of strings, and electrical specifications. To ensure optimum system performance, battery autonomy must be sufficiently efficient to provide electrical power to the station during disruptions of the main power source caused by weather conditions until the power source is restored. System 2 demonstrates the greatest degree of autonomy, followed by Systems 4, 3, and 1.

As stated previously, minimizing the weight of the batteries is essential because a lighter weight facilitates the relocation of the station. In ascending order of weight, System 1 is the lightest at 560 kg, followed by System 3 at

672 kg, System 4 at 1,128 kg, and System 2 at 1,504 kg, the latter being the precise inverse of system independence.

The area of each system should be considered due to its importance in assembly and resistance to weather influences, ensuring an exact comparison of all systems (Table 6).

System 1 has the largest area (around 40 m²), followed by System 3 (around 36 m²), System 4 (32 m²), and System 2 (30 m²).

In conclusion, System 3, 6.19 kW, is the lightest, exhibiting a weight difference of 456 kg from the subsequent system and being roughly \$1,340 cheaper than the system that follows it.

Table 5. Specification of 24 and 36 V battery bank connection system

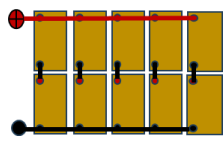
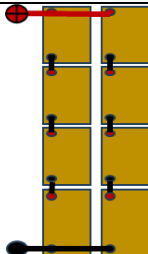
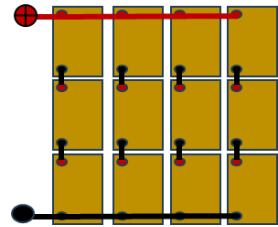
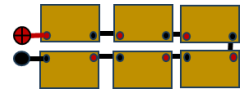
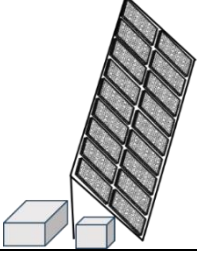
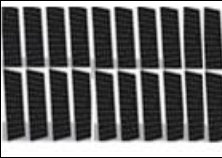
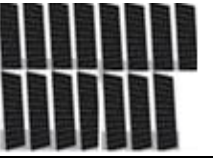
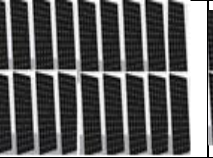
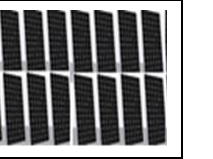
	24 V System		36 V System	
System no.	1	2	3	4
PV size	7.31 kW	5.17 kW	6.19 kW	5.67 kW
Battery bank connection type				
Station size	7.31 kW	5.17 kW	6.19 kW	5.67 kW
Item	Trojan 12 255	SIND 6 1225	Trojan 12 255	SIND 6 1225
Batteries (qty)	10	8	12	6
String size	2 batteries	4 batteries	3 batteries	6 batteries
Strings in parallel	5 strings	2 strings	4 strings	1 string
Bus voltage	24 V	24 V	36 V	36 V
Nominal capacity	30.9 kWh	60.9 kWh	37.1 kWh	45.6 kWh
Autonomy	39.8 h	78.4 h	47.7 h	58.8 h
Batteries' total weight	$56 \times 10 = 560$ kg	$188 \times 8 = 1,504$ kg	$56 \times 12 = 672$ kg	$188 \times 6 = 1,128$ kg

Table 6. Winning system specifications

PVs, battery bank, and DC inverter			Station size after installation: PV panels, 4m height \times 10 m (H \times W) • Inverter and batteries: 1.5 m \times 1 m \times 0.5 m (L \times W \times H) • Batteries: 1.5 m \times 1 m \times 0.5 m (L \times W \times H)	
	24 V System		36 V System	
System no.	System 1	System 2	System 3	System 4
PV size	7.31 kW	5.17 kW	6.19 kW	5.67 kW
PV model: SG360M				
PV weights (number of PV \times weight)	20 \times 22 kg = 440 kg	15 \times 22 kg = 330 kg	18 \times 22 kg = 396 kg	16 \times 22 kg = 352 kg
Total PV area (H \times W)	2 \times 1 \times 20 = 40 m ²	2 \times 1 \times 15 = 30 m ²	2 \times 1 \times 18 = 36 m ²	2 \times 1 \times 16 = 32 m ²
Apollo S-219Cia	114 kg (Inverter weight)			
Total system weight	1,114	1,948	1,182 kg	1,594
Total net present cost	\$14,474	\$18,125	\$14,696	\$16,036

5. Results and Discussion (System no 3- 6.19 kW)

5.1. PV Power Output

The PV output of the mobile MEV charging station shown in Figures 8 and 9 covers a one-year period (2025). According to HOMER results and the PV output density map, the PV array had a reasonably stable power production from February to October, reaching around 6 kW. However, on

some days, the PV arrays experience low energy production, particularly from November to the end of February or the beginning of March. Although the PV array specification illustrates a 6.19 kW rated output capacity, this system has a maximum PV output of 6 kW, with a total of 10,664 kWh/year (Table 7). Based on the information provided by HOMER, the system is expected to deliver the lowest amount of energy on March 6, 2025, which could lead to an energy deficit, with recovery projected within three days.

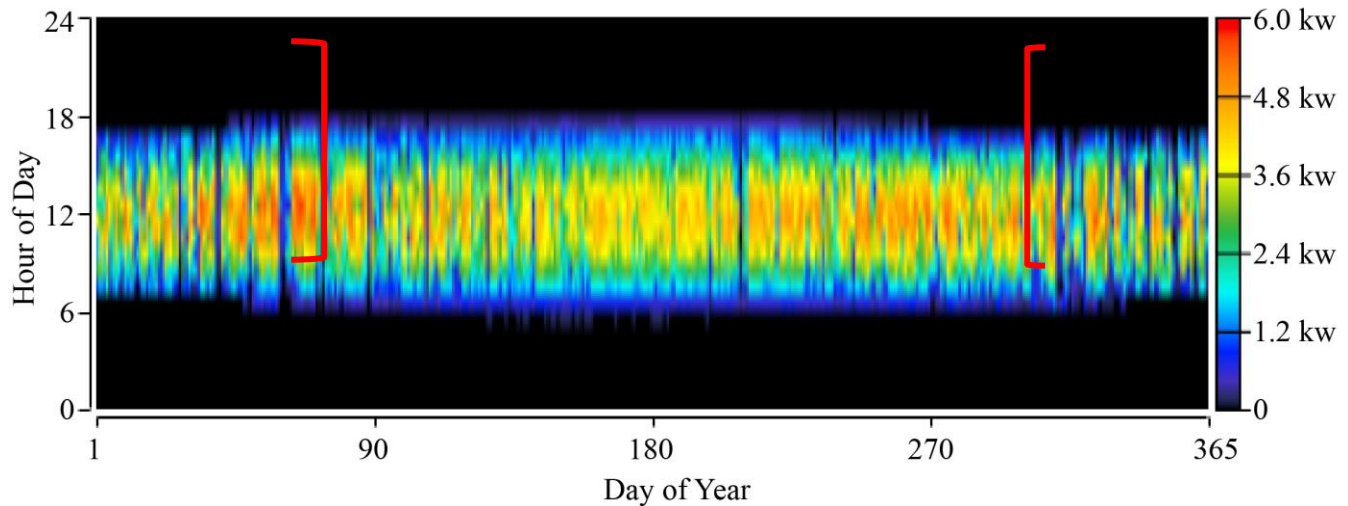


Fig. 8 One-year daily PV output for portable MEV charging station in Kuwait (a significant drop in energy production may occur from November until early March)

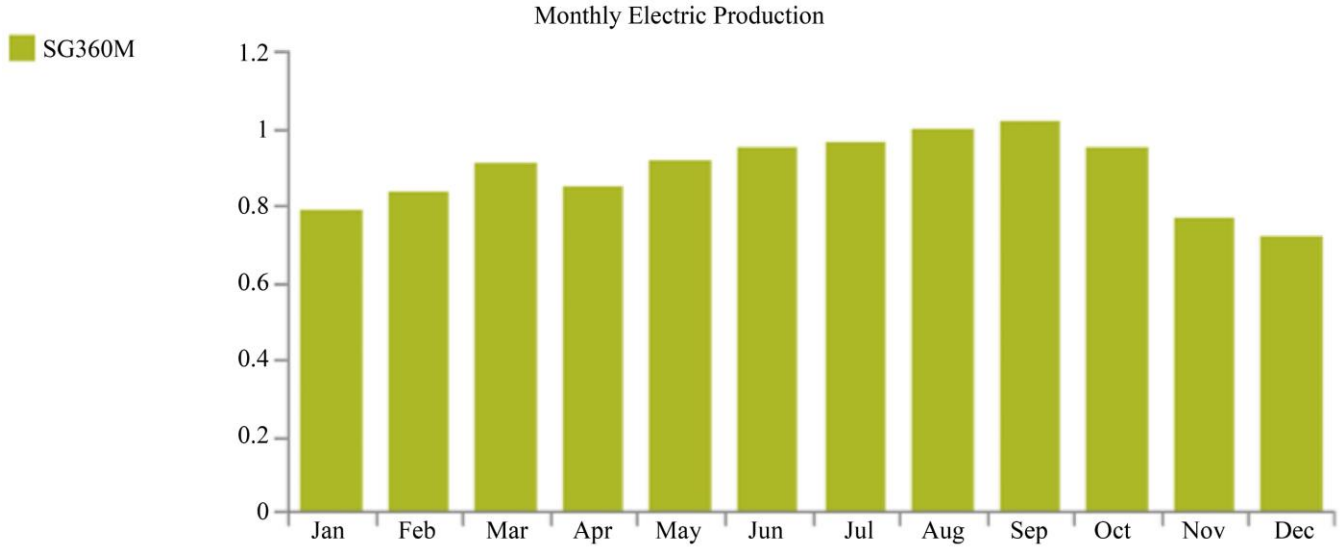


Fig. 9 Monthly energy production

Table 7. PV electrical production

Production	kW/y	%
Peimar SG360M	10,504	100
Total	10,504	100

5.2. Total Loads Served (AC and DC Primary Loads)

The AC primary load in Figure 10 represents the EV charging load, while Figure 11 illustrates the DC primary load required to operate the system and its equipment (e.g., illumination, monitoring). The EV charging time aligns with the PV peak energy production time, commencing at 8:30 a.m. and concluding at 4:30 p.m. throughout the year.

The total station capacity can reach 6,460 kWh per year. The annual charging energy is approximately 15,200 kWh per day or 5,548 kWh per year. The estimated daily charging power is 10.5 kW, which is sufficient to recharge the depleted

batteries of a vehicle with a 10 kW engine, allowing it to travel a distance of 90 km.

The DC primary load is anticipated to operate continuously for 24 hours and exhibits fluctuations between 0.05 and 100 W/h, resulting in a total of 912 kWh per year. Additional energy consumption may be required to ensure the station's safety and illuminate it at night so that others are aware of it and to prevent fatalities.

Table 8. System loads

Consumption	kW/Year	%
AC Primary Load	5,548	85.9
DC Primary Load	912	14.1
Deferrable Load	0	0
Total	6,460	100

Daily Profile

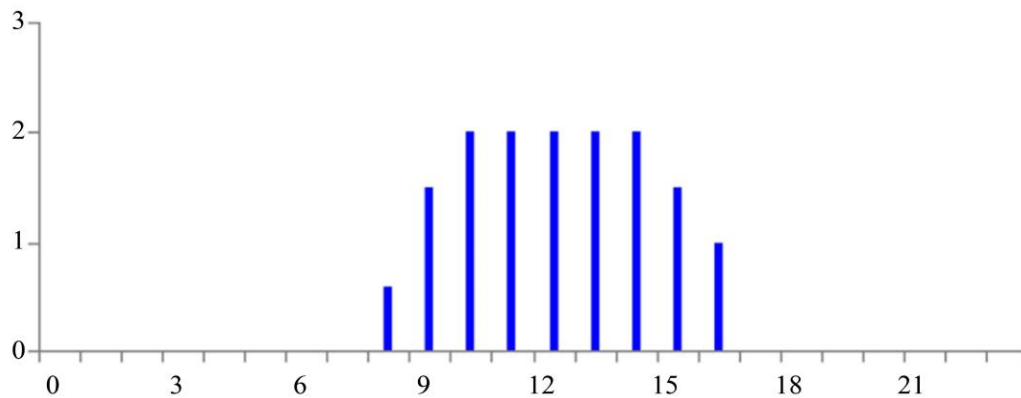


Fig. 10 Primary AC load served

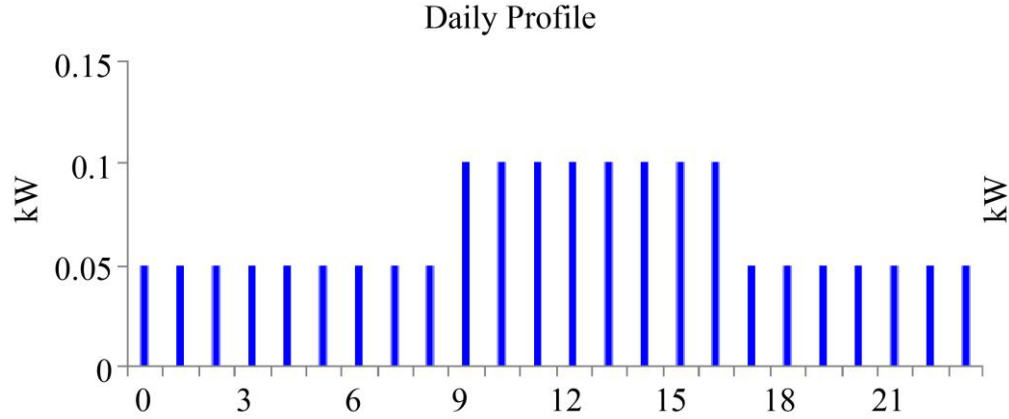


Fig. 11 DC primary load

5.3. State of Charge 15.2 kW (12 Batteries - SSIG 12 255)

The expectation for the PV output 2025 is determined by the HOMER sensitivity results, which also presume the state of charge. The portable solar EV station's charge density map for the daytime hours of one year is depicted in Figure 9. During most of the year, the map illustrates the battery charge status of the station.

For a period of 10 months, the station's state of charge varied from 60% to 100% during the day. Moreover, the state of charge fluctuated below 60% for around two months, and the total number of days with an energy shortage was less than two weeks throughout the year. The figure depicts a decrease in the number of states during the months of January, February, November, and December, with February and November being the most critical periods. The charging state of the system is at its most optimal during the early hours of the day, suggesting that it is capable of charging electric vehicles in the early morning.

It also demonstrates that the system is capable of coping with a decrease in solar energy in the event of a shortage of PV solar power. However, as previously mentioned, there are occasions when the batteries are not fully charged, requiring larger batteries with a nominal capacity of 37.1 kWh and an autonomy of 47.7 hours.

These batteries are designed to accumulate electrical energy in advance of any anticipated shortfalls. This energy deficit, less than 20%, occurs over a few days from November to approximately March 10. Nevertheless, the design can satisfy the electrical energy requirements for charging MEVs.

To ascertain the surplus in electrical energy, the excess electrical energy generated needed to be evaluated to ascertain the size of the solar panels and whether they would satisfy the system's requirements. Thus, the following sections investigated the excess electrical energy.

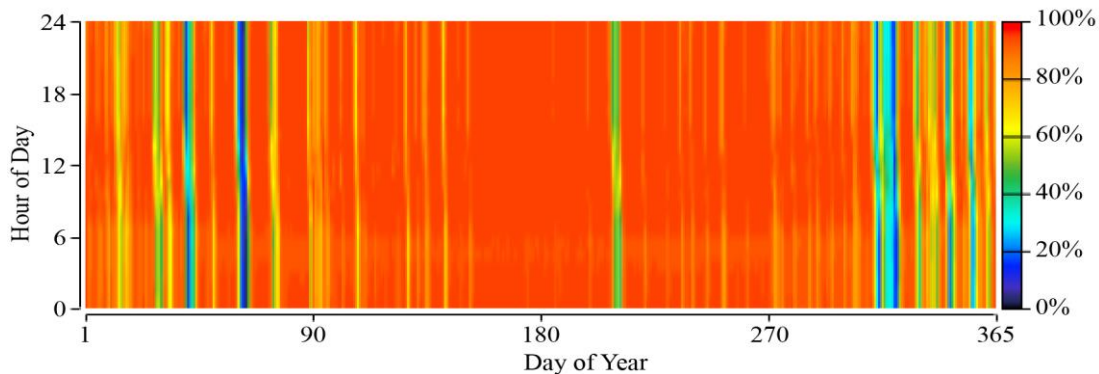


Fig. 12 HOMER sensitivity results for the state of charge of station batteries

5.4. PV Over Production (Excess Electricity)

The HOMER sensitivity results for the excess electricity generated by the system are depicted in Figure 13, which includes a density map and graph line. The total excess electricity amounts to 3,700 kW/year, approximately 34.7%

of the total production (Table 9). Regardless of the fact that there is a monthly excess of electricity, the system may still experience a shortfall in electricity production during consumption.

In accordance with the earlier data, it appears that the excess electricity will be reduced from the middle of November to early March, as indicated by the black area in the density map. Furthermore, the figure indicates that the system's utility requirements may be significantly insufficient during these months.

The electricity shortage is not just related to the reduction in electrical energy production; it may also be the result of a continuing decrease in electrical production. PV output production experienced its lowest level of the year in December; however, it can still meet the system's demands. Nonetheless, HOMER demonstrated a relatively greater PV electricity output in March than in December. However, the

system failed to completely meet the electricity requirements in some ways.

Consequently, PV electrical production shortages may arise in any month of the year, depending on weather conditions, even if there is an excess of electricity production in that month. This situation results in battery depletion, as the system is unable to recharge the batteries and cover the charging of electric vehicles during working hours. HOMER predicted an electricity demand deficit of up to 5.5 kW per year, equivalent to approximately 0.085% of the total station consumption. Additionally, the station's performance is not affected by an unmet electrical demand of up to 0.6 kW per year, which is as low as 0.009% of the total consumption.

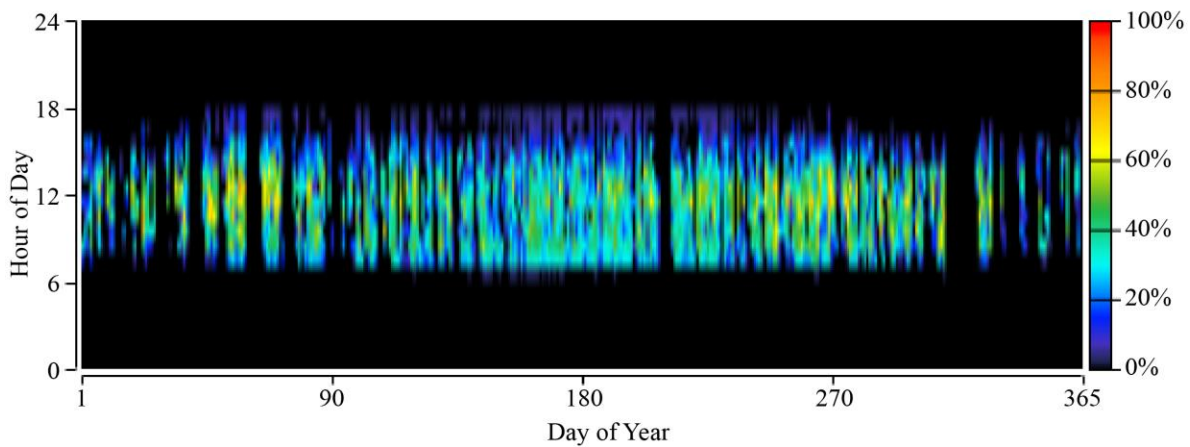


Fig. 13 Overproduction of electricity: density map
Excess Electrical Production Daily Profile

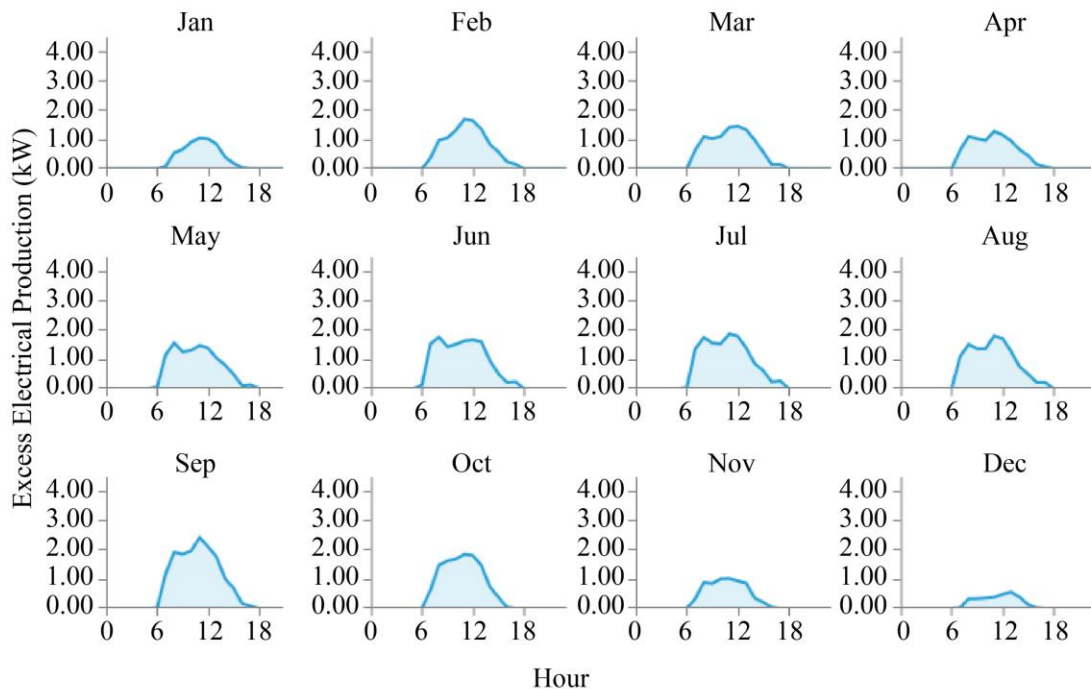


Fig. 14 Monthly surplus of generated electricity

Table 9. System overproduction electricity

Excess Electricity	kW/year	%
Excess Electricity	3,591	34.2
Unmet Electric Load	0.45	0.007
Capacity Shortage	4.28	0.0662

6. Discussion

6.1. System Performance

This section analyzes the station's performance by comparing the results. Figure 15 illustrates the station's performance during the year 2025. The upper chart illustrates a comparison between the performance of solar panel production and the non-compensated load, while the lower chart compares the battery charging state and the total load served during the same year, as it helps in comparing all the results.

An examination of the performance of solar panels shows several instances in which the production energy is significantly reduced, leading to a dependence on battery power. The system's efficacy and reliability are demonstrated by the utilization of batteries to meet the station's energy requirements. Nevertheless, there are certain days of the year

when energy production can decrease, resulting in protracted battery consumption and a disruption in the station's performance. The energy deficit graph demonstrates that the system could not fulfil the requisite electrical needs, as shown by a small rise.

To conduct a more precise analysis of the system, we proceed to the lower diagram, which shows the performance of the serviced loads and the batteries. The most significant factor that demonstrates the station's performance is the status of the battery charge, as the graph displays fluctuations in battery energy over the course of the year. This finding suggests that the station's performance is satisfactory, as the charge level is consistently above 20% for the majority of the year.

Nevertheless, the energy stored in the batteries declined substantially at the start and the end of the year (during winter). The lowest levels are observed in November, while the greatest shortfall is observed at the beginning of March, contrasting with the shortfall in load coverage in the upper graph. Figure 15 displays the station's performance for the duration and period to facilitate a more effective analysis of the deficiencies that occurred in March.

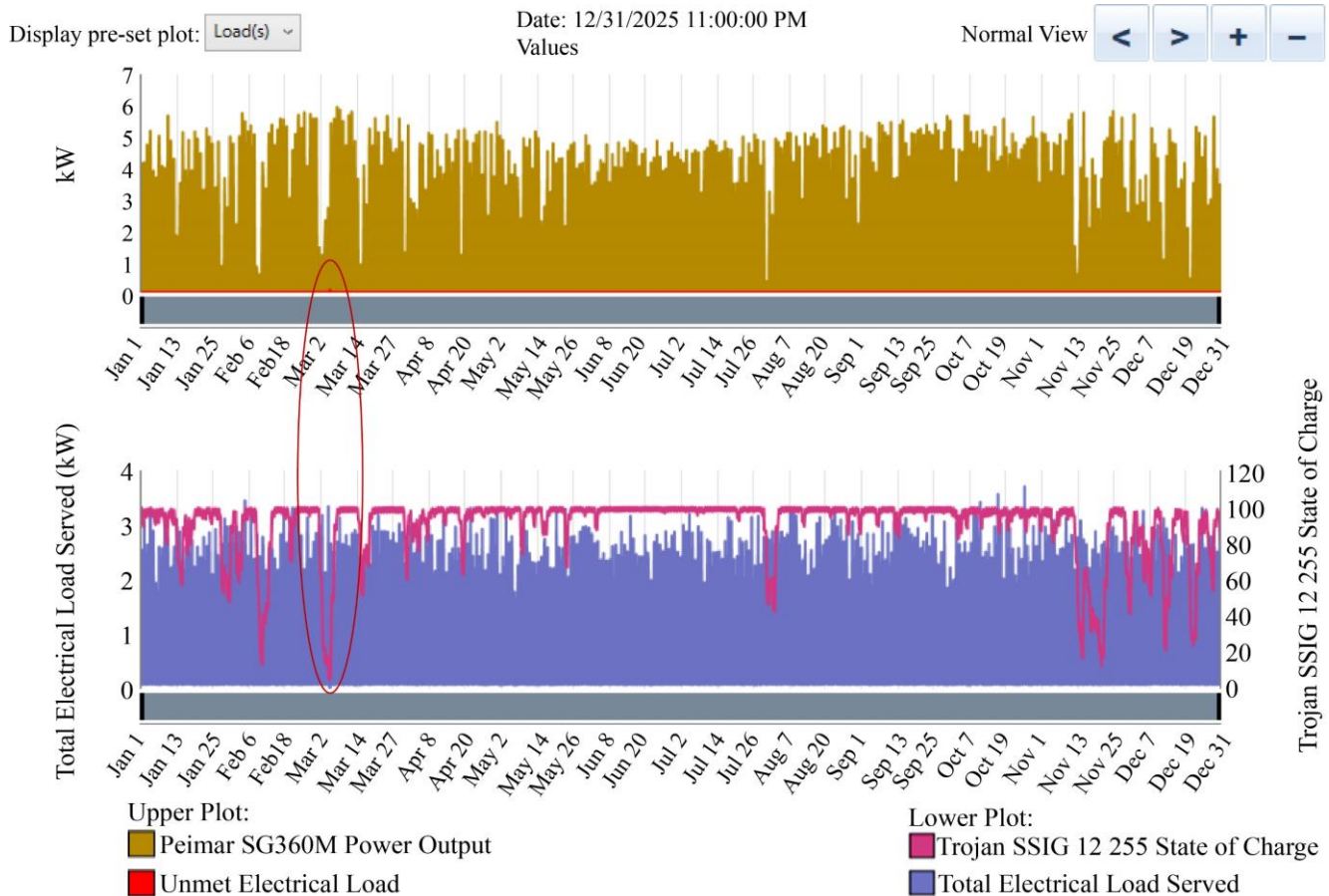


Fig. 15 PV output, unmet electrical load, state of charge, and total load served (the figure shows the lowest production energy time)

Figure 16 illustrates the station's performance in March, particularly during the March 6, 2025 energy decline. The HOMER results indicate that the energy shortfall occurred during a single day, as the battery charge level fell below 20%, while the energy demand was 0.5 kWh/year. (The energy demand slightly exceeds the electrical load served, making it inadequate for charging.)

Fortunately, the decline in energy was limited and short, as shown by the findings at the end of the day. The next day, the system promptly achieved a 40% charge, and within three days, the charging status reached 100% on March 9, ensuring the anticipated performance of the station.

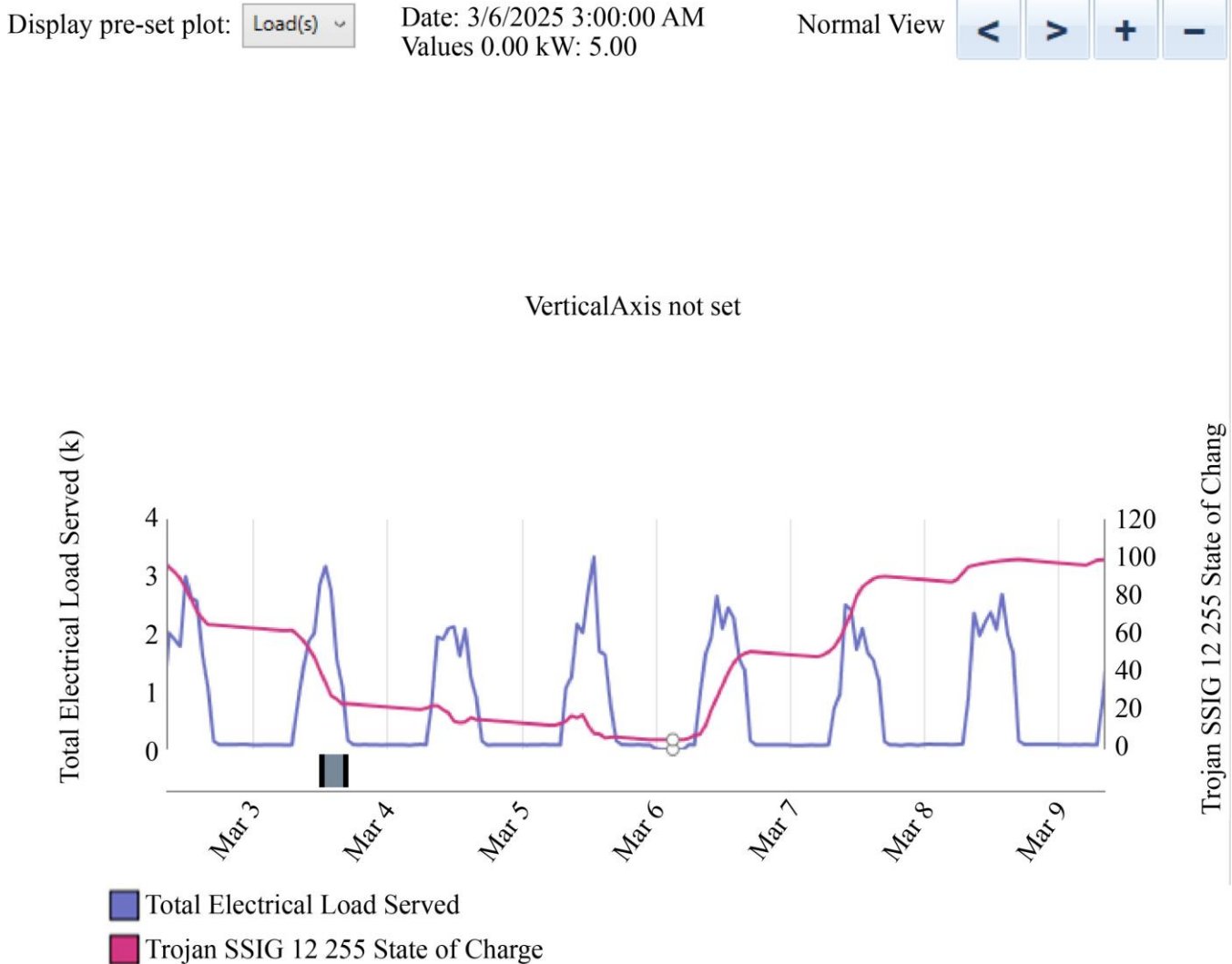


Fig. 16 Critical energy shortfall on March 6

6.2. System Economics

The station's initial capital cost was \$12,565; 44% of this was allocated to the battery bank (Trojan SSIG 12-255), 32% to PV expenditures, and 23.8% to inverter expenses (Leonic S-219) (Figure 17). The system requires additional operational expenditures and replacements during the station's lifetime. After 10 years, the inverter experienced the highest regular expenses, with a replacement cost of about 21% (\$2,650) and a total salvage of \$519.92 for the inverter and battery bank. (Salvage is the value that remains in a component at the end of the project's life span, as defined by

HOMER). The EV station is capable of operating for more than 25 years; however, in this study, it is suggested that the station be operational for 15 years. Therefore, HOMER did not calculate any maintenance or operating costs beyond this period, resulting in a total net present cost of \$14,696.

HOMER determined that the electrical cost over the system's lifetime is \$0.1767/kW, thereby attaining sustainability and zero greenhouse gas emissions without any infrastructure requirements (Table 10).

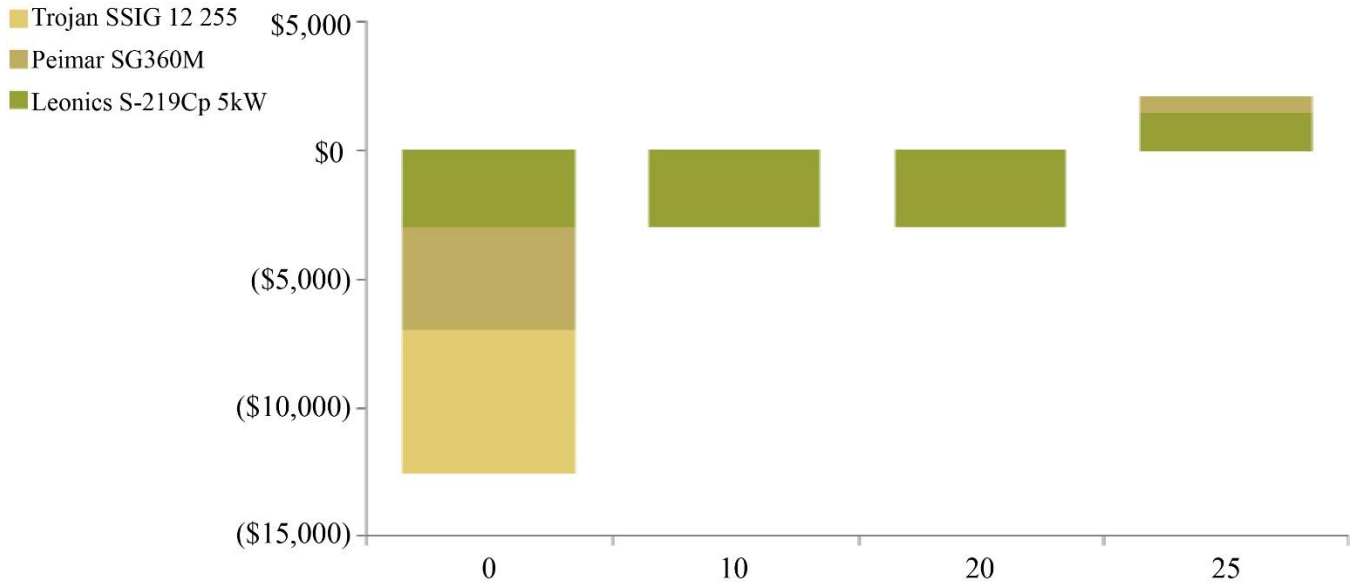


Fig. 17 System operation and replacement expenses

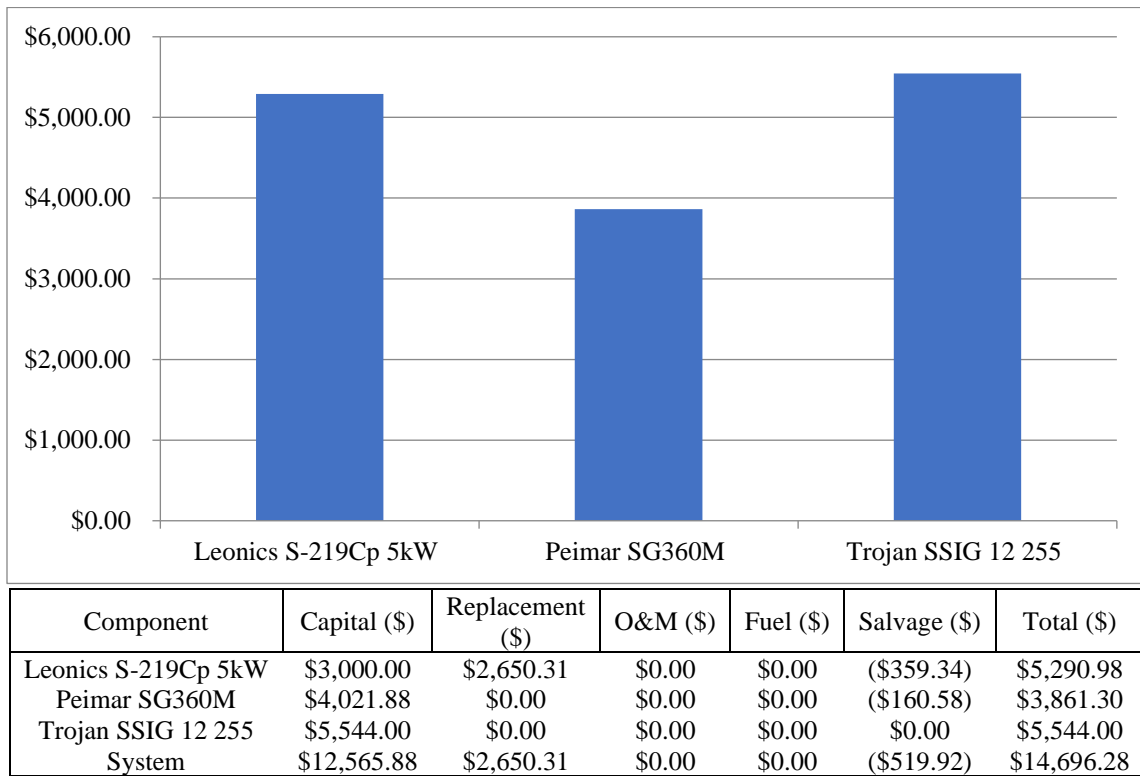


Fig. 18 System's initial capital and total net present cost

Table 10. Emissions

Quantity	Carbon Dioxide	Carbon Monoxide	Unburned Hydrocarbons	Particulate Matter	Sulfur Dioxide	Nitrogen Oxides
Value kg/yr	0	0	0	0	0	0

7. Conclusion

In this study, the mobile solar charging station for MEVs, unlike traditional charging stations, demonstrated its potential to support sustainable transportation in remote and rural areas of Kuwait, aligning with the national goals of pollution reduction and renewable energy integration. By optimizing the system design using HOMER simulation software, we identified the most efficient configurations in terms of energy output, battery autonomy, station weight, and installation area, ensuring that the station is cost-effective, environmentally friendly, and practical for on-the-ground deployment.

The results confirmed that the use of solar energy, particularly in Kuwait's high-solar-radiation climate, provides a reliable source of electricity for charging MEVs, minimizing the reliance on grid power and fossil fuels. The station's portability offers a significant advantage, as it can be easily transported and installed in various locations, making it ideal for rural farms, islands, and other remote areas where fixed infrastructure is limited or unavailable. Additionally, the excess energy produced by the system, particularly during peak solar months, offers opportunities for further grid integration and the potential to sell surplus energy, enhancing the overall economic viability of the system.

The study also highlighted key technical considerations, such as the importance of balancing battery size, weight, and capacity to optimize performance while ensuring that the station remains portable.

The flexibility of different system configurations allows for customization based on specific site requirements, offering scalability to larger or smaller installations depending on energy needs.

Overall, the mobile solar charging station offers a promising solution to address the lack of electric vehicle charging infrastructure in remote regions. By supporting the use of MEVs and promoting the adoption of renewable energy technologies, the system contributes to both environmental sustainability and economic development.

Future work could explore the integration of additional renewable energy sources, advancements in battery technology, and the long-term performance of the station under various environmental conditions, ensuring continued improvements in system efficiency and cost-effectiveness.

References

- [1] Top 5 Sports Car Trends in Kuwait for 2024, 4Sale, 2024. [Online]. Available: https://www.q84sale.com/en/blog/automotive/top-5-sports-car-trends-in-kuwait-for-2024?srltid=AfmBOoqzA4KD3WhyDopUqVbnP5eU4hGoZu0LM_KCuoZeA-DXF9IADsp
- [2] Speedways Electric: If you can Dream it, We can Make it, 2024. [Online]. Available: <https://speedwaysev.com/about-us>.
- [3] Ali Jawad Alrubaie et al., "A Comprehensive Review of Electric Vehicle Charging Stations with Solar Photovoltaic System Considering Market, Technical Requirements, Network Implications, and Future Challenges," *Sustainability*, vol. 15, no. 10, pp. 1-26, 2023. [CrossRef] [Google Scholar] [Publisher Link]
- [4] Prabuddha Chakraborty et al., "Addressing the Range Anxiety of Battery Electric Vehicles with Charging en Route," *Scientific Reports*, vol. 12, no. 1, pp. 1-15, 2022. [CrossRef] [Google Scholar] [Publisher Link]
- [5] Apollo S-210 ia: Single Phase Grid Interactive Inverter, LEONICS, 2024. [Online]. Available: <https://cdn.enfsolar.com/z/pp/2023/10/qlv8pnnw4f49jf/S-210ia-183.pdf>
- [6] Yonis Gulzar et al., "Revolutionizing Mobility: A Comprehensive Review of Electric Vehicles Charging Stations in India," *Frontiers in Sustainable Cities*, vol. 6, pp. 1-14, 2024. [CrossRef] [Google Scholar] [Publisher Link]
- [7] Stanton W. Hadley, and Alexandra A. Tsvetkova, "Potential Impacts of Plug-in Hybrid Electric Vehicles on Regional Power Generation," *The Electricity Journal*, vol. 22, no. 10, pp. 56-68, 2009. [CrossRef] [Google Scholar] [Publisher Link]
- [8] PEIMAR, 2024. [Online]. Available: http://tp.com.ht/attachment_pdf/peimar/SG360M/SG360M%20Data%20Sheet.pdf .
- [9] Homer Software, ULTRUS, 2024. [Online]. Available: <https://homerenergy.com/index.html>
- [10] Global EV Outlook 2024, IEA, 2024. [Online]. Available: <https://iea.blob.core.windows.net/assets/a9e3544b-0b12-4e15-b407-65f5c8ce1b5f/GlobalEVOutlook2024.pdf>
- [11] Wei Jiang, and Yongqi Zhen, "A Real-Time EV Charging Scheduling for Parking Lots with PV System and Energy Store System," *IEEE Access*, vol. 7, pp. 86184-86193, 2019. [CrossRef] [Google Scholar] [Publisher Link]
- [12] Saadullah Khan et al., "A Comprehensive Review on Solar Powered Electric Vehicle Charging System," *Smart Science*, vol. 6, no. 1, pp. 54-79, 2018. [CrossRef] [Google Scholar] [Publisher Link]
- [13] Electric Car Chargers' Regulation Ready- Kuwaiti Official, Kuna.net.kw, 2022. [Online]. Available: <https://www.kuna.net.kw/ArticleDetails.aspx?id=3052594&language=en#>
- [14] Ziwen Ling, Christopher R. Cherry, and Hongtai Yang, "Emerging Mini Electric Cars in China: User Experience and Policy Implications," *Transportation Research Part D: Transport and Environment*, vol. 69, pp. 293-304, 2019. [CrossRef] [Google Scholar] [Publisher Link]

- [15] Elżbieta Macioszek, and Grzegorz Sierpiński, *Research Methods in Modern Urban Transportation Systems and Networks*, 1st ed., Lecture Notes in Networks and Systems, Springer Cham, 2021. [[CrossRef](#)] [[Google Scholar](#)] [[Publisher Link](#)]
- [16] More than a Golf Cart: Alke' Electric Golf Car, Alke, 2024. [Online]. Available: <https://www.alke.com/electric-car-golf>
- [17] Pedro Nunes, Raquel Figueiredo, and Miguel C. Brito, "The Use of Parking Lots to Solar-Charge Electric Vehicles," *Renewable and Sustainable Energy Reviews*, vol. 66, pp. 679-693, 2016. [[CrossRef](#)] [[Google Scholar](#)] [[Publisher Link](#)]
- [18] SSIG 12 255 12V Flooded Lead Acid Battery, TROJAN, 2024. [Online]. Available: <https://www.trojanbattery.com/products/ssig-12-255-12v-flooded-battery>
- [19] Trojan, SIND 06 1225, 2024. [Online]. Available: <https://www.trojanbattery.com/search?query=SIND+06+1225&refinementList=%5B%5D&page=1>
- [20] Xu Yidan et al., "State of Charge Estimation for Lithium-Ion Batteries Based on Adaptive Dual Kalman Filter," *Applied Mathematical Modelling*, vol. 77, no. 2, pp. 1255-1272, 2020. [[CrossRef](#)] [[Google Scholar](#)] [[Publisher Link](#)]